JURNAL rekayasa mesin
ISSN 2477-6041 articles 13, pp. 513 – 524, 2023
Vol. 14. No.2

INDUCED DRAFT FAN DOMINANT FREQUENCY DETECTION USING SHORT-TIME FOURIER TRANSFORM METHOD

Dedik Romahadi [1,2] ✉, Wiwit Suprihatiningsih [1], Gian Villany Golwa [1], Mahesh Kumar [2]

[1] **Mechanical Engineering**
Universitas Mercu Buana
dedik.romahadi@mercubuana.ac.id
wiwit.suprihatiningsih@mercubuana.ac.id
gianvgolwa@mercubuana.ac.id

[2] **Mechanical Engineering**
Beijing Institute of Technology
3820222029@bit.edu.cn

Abstract

Weak suction and large vibrations indicate an Induced Draft Fan (IDF) problem. The Fast Fourier Transform (FFT) method cannot be applied to non-stationary vibration signals. Therefore, this study aims to analyze non-stationary vibration signals for IDF vibration signals at start-up so that the source of damage to the IDF can be found. The research process begins with a brief measurement of both bearing locations with horizontal and axial axes. Processing of the vibration signal from the measurement using the FFT method and the Short Time Fourier Transform (STFT). Based on the STFT spectrogram graph for measurements on the horizontal and axial axes, the dominant frequency values are the same. The frequency with the largest amplitude value is at one RPM IDF or 25 Hz. High vibration at 1 RPM is a big indication that the IDF is experiencing unbalance.

Keywords: *Vibration Analysis, Induced Draft Fan, Analysis Vibration, STFT, FFT.*

1. INTRODUCTION

The Induced Draft Fan (IDF) is an important component of the combustion system in the boiler. IDF plays an important role in circulating air during the combustion process [1]. IDF which functions to maintain pressure in the boiler furnace and works at low atmospheric pressure to suck gas and ash from combustion in the boiler for further disposal through the stack. Decreased suction power of the IDF and the appearance of high vibrations indicate a problem has occurred. This can be an indicator of a mechanical problem or cause other problems if the vibration reaches a certain amplitude. Large vibrations in the IDF can reduce performance and shorten the life of IDF components. The vibrations generated by the IDF are caused by minor defects in the rotating parts. The most common defect is that the center of gravity does not coincide with the center of rotation or is called "unbalance" [2].

Condition monitoring the most effective solution for predictive maintenance of machines and minimizes unplanned failures and potential downtime. In addition to increasing plant availability and efficiency in industrial safety [3]. Vibration analysis method that works in predictive maintenance [4], [5]. Vibration frequency characteristics reveal most types of damage. Vibration analysis is an effort to reduce damage to machine components that spread to other machine components [6]–[8]. Impact vibration measurement allows for faster and more accurate fault detection [9], [10]. Signal processing techniques time domain statistical analysis and Fourier transform methods used for signal analysis and fault diagnosis

Corresponding Author:
✉ **Dedik Romahadi**
Received on: 2022-07-18
Revised on: 2023-05-04
Accepted on: 2023-06-25

DOI: 10.21776/jrm.v14i2.1305

[11]. Damage to the machine is reflected by frequency, or the time frequency domain is used to extract features [12].

Basically the use of the FFT method has the disadvantage of being inefficient in describing non-stationary signals caused by vibration signals [13] and the limited range of transformable waveform data due to the need for time-frequency representation. So, the STFT method is needed by using a window or windowing signal to process data signals from time to time.

Previous research conducted by Mateo and Talavera discussed the application of STFT using the MATLAB application but did not apply it directly to the engine vibration signal [14]. Furthermore, Dutta et al only determined the damage and was not equipped with the condition of the problematic unit condition according to the spectrum analysis in the ISO 10816-3 vibration analysis standard [15]. Next, Vippala et al's research applied the FFT method to monitor the condition of the Brushless DC (BLDC) motor but it was not equipped with results from the measurement variation point during vibration analysis [16]. In addition, research conducted by C. T. Alexakos et al discusses the application of STFT for image processing of hot bearings [17].

It is necessary to develop the ability to analyze in the low and medium frequency range the measurement of non-stationary vibrations originating from a rotating machine using a vibration sensor. This research is based on previous research quoted from references [18]. STFT can be defined as the subject of spectrum analysis using FFT, short signal sequences are treated as quasi-stationary. The division of the input signal into segment analysis is implemented using a technique called a moving window [19] stated that the application of STFT as a time frequency method, which can provide more information about the signal in time and frequency.

In this case, the researcher conducted a research process using STFT on the detection of the dominant frequency of IDF in accordance with the ISO 10816-3 vibration analysis standard. It is hoped that this research will be able to extract information from the results of vibration measurements on the IDF in the case of non-stationary signals obtained by vibration sensors mounted on horizontal and axial bearing positions during engine start-up. The extracted information can be used to support a more detailed post or real-time vibration diagnosis of the IDF during the operating state by providing preprocessed basic time-frequency information.

2. MATERIAL AND METHOD

2.1. Fast Fourier Transform

FFT is a mathematical operation calculation technique used to transform analog signals into frequency-based digital signals [7]. FFT divides a signal into different frequencies in a complex exponential function. FFT calculates discrete Fourier transforms quickly and efficiently. Because the signals in the communication system are continuous, the results can be used for Fourier transforms. Fourier Transform can be defined by Equation (1) [20]

$$F = \frac{1}{N}\sum_{n=0}^{N-1}[X]\cdot e^{-j2\pi(n-1)k} \quad (1)$$

Where N is the number of time samples, X is the signal in the time domain, n is the time sample series and k are the result of dividing each time sample by the number of time samples. Calculating this series directly requires O(N2) arithmetic operations. An FFT

algorithm requires only O(N log N) operations to compute the same series. In general, the algorithm depends on factoring N.

2.2. Short Time Fourier Transform

STFT can be applied to both stationary and non-stationary signals. The time domain signal is divided into small windows of equal length using the windowing function and then the FFT method is applied, which provides a time-frequency spectrum [21].

$$w(n) = 0.5\left(1-\cos\left(2\pi\frac{n}{N}\right)\right), \quad 0 \le n \le N \tag{2}$$

In this analysis, the Hanninging windowing function as shown by Equation (2) is applied to obtain time-frequency information. The shape of the Hanninging window is shown in Figure 1. The length of the window is L=N+1. The STFT concept can be seen in Figure 2, which explains the process of processing the vibration signal to become a spectrogram graph. In the case of discrete time, the data to be transformed can be broken down into chunks or frames (which usually overlap each other, to reduce artifacts at the boundary). Each slice is Fourier transformed, and the complex result is added to the matrix, which records the magnitude and phase for each point in time and frequency [22]. The number of columns in the STFT matrix is given by Equation (3).

$$k = \left\lfloor \frac{N_x - L}{M - L} \right\rfloor \tag{3}$$

Where Nx is the original signal length x(n) and the symbol in brackets denotes the floor function. The number of rows in the matrix is equal to the NFT, the number of points of the Fourier Transform (FT), for the center and two-sided transformations and ⌊NFT/2⌋ + 1 for a one-sided transformation. The STFT matrix is given by Equation (4). So, the Mth element of this matrix is generated by Equation (5).

$$X(f) = \left[X_1(f)\ X_2(f) \cdots X_k(f) \right] \tag{4}$$

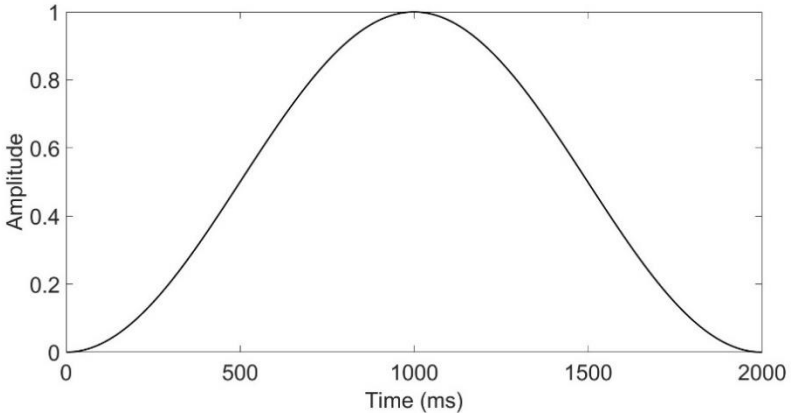

Figure 1. Hanninging Window

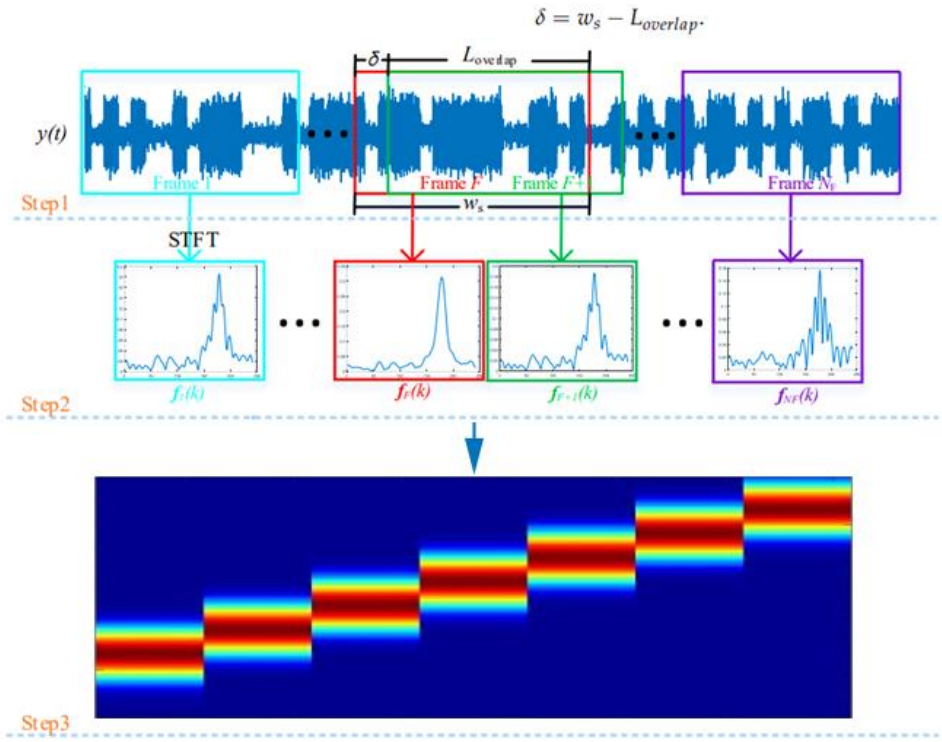

Figure 2. The flow chart of the STFT

Where, g(n) is a window function of length M. Xm(f) is the FT of the window data centered on time mR. R is the hop size between successive FTs. The hop size is the difference between the window length and the overlap length L. Usually in STFT applications it is done on a computer using a fast Fourier transform, so that both variables are discrete and quantized. [23].

$$X_m(f) = \sum_{n=-\infty}^{\infty} x(n)g(n-mR)e^{-j2\pi fn} \tag{5}$$

The data processing process is as shown in Figure 3, which begins with preparing measuring instruments. Vibration measurements on the IDF are carried out in the horizontal and axial bearing positions using an accelerometer-type vibration sensor. The measured vibration signal is then processed using STFT-based MATLAB software with the aim of showing the dominant frequency value. Analysis of the source of the problem in the IDF by utilizing detailed vibration data, time domain data, time frequency domain, Pre Hanning window, Hanning window, Applied Han Window, and Fourier transform spectrogram by applying FFT and STFT. Then the data analysis is carried out so that it can find out the condition and location of the IDF damage.

Figure 3. The processing scheme of vibration signal

2.3. IDF Specification

The position of the vibration measurement is carried out at the DE Fan location. Each with a horizontal and axial direction. Measurements are carried out directly by attaching the accelerometer transducer to each bearing location using a vibration measuring tool called Vibexpert II. At the stage of taking vibration data at the beginning of the start-up of IDF operation, data collection is carried out, namely in the axial and horizontal positions using an accelerometer that is attached to the outside of the bearing, with the scheme in collecting IDF vibration data as shown in spectrogram Figure 4.

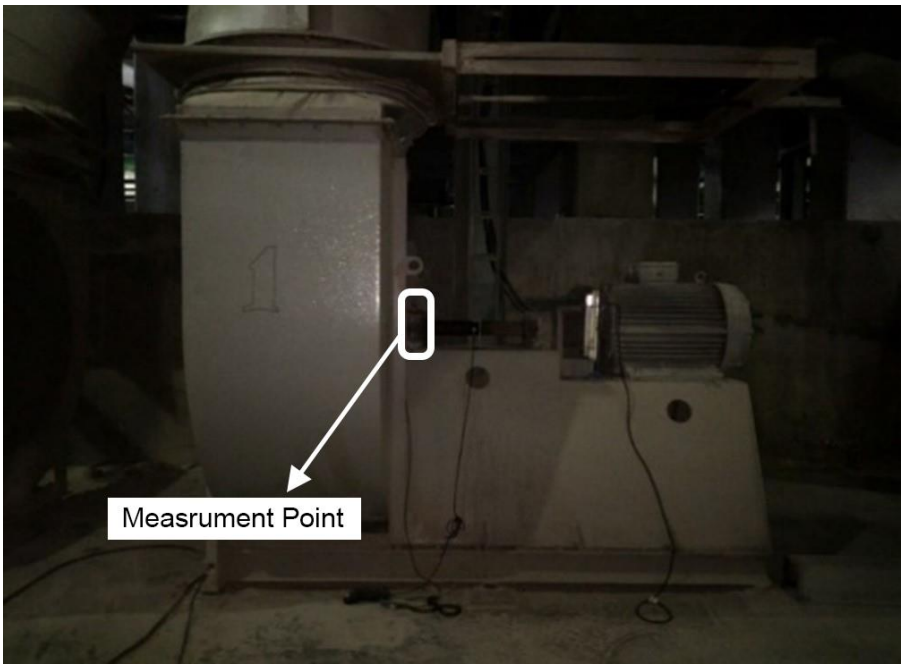

Figure 4. Blower C3a (IDF)

In this study, the machine used is an IDF named Blower C3a with an electric motor connected via a shaft and a coupling type coupling, as shown in Figure 4. IDF has the following specifications,

Name	: Blower C3a
Power	: 75 kW
Foundation	: Flexible
Motor Speed	: 1500 RPM
Diameter Impeller	: 900 mm
Rotor Weight	: 250 kg
Transmission System	: Coupling

2.4. Vibration Signal from Measurement

The results of signal processing using the MATLAB application obtained from the results of measuring the vibration signal according to the axial and horizontal axes as shown in Figures 5 and 6. Figure 5 is the time domain on the axial axis where the results of the vibration data retrieval are carried out at the beginning of start-up. up operation which takes five seconds of vibration with many samples with a frequency of 4096. It can be seen in the graph that the largest amplitude has a value of 2.5 mm/s RMS. The IDF vibration signal has a small amplitude and frequency at the start of operation and gets bigger as the IDF motor rotates faster.

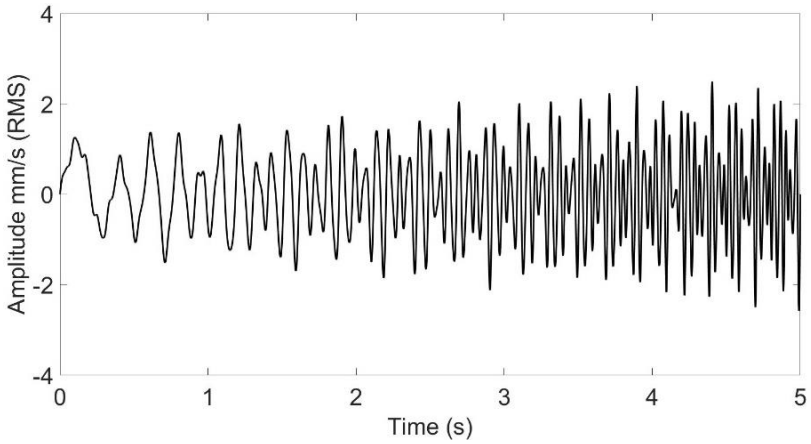

Figure 5. Axial time signal

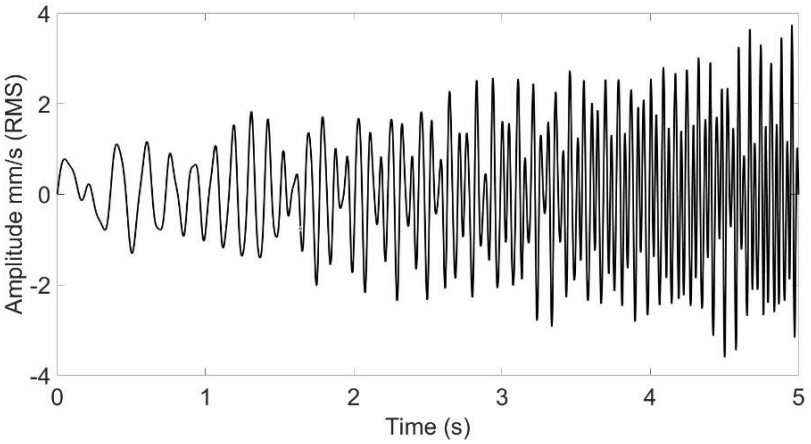

Figure 6. Horizontal time signal

The many sources of non-stationary vibrations generated by the Fan ID components in the time domain graph make it difficult to locate the frequency of an amplitude. Using a time domain graph has limitations in reading the frequency of the vibrations that appear. The time domain graph shows only the amplitude and time values of the measurements. The vibration signal measurement data at the horizontal point that has not been processed or is still in the time domain is shown in Figure 6. It can be seen that the farthest amplitude deviation is 3.7 mm/s RMS. The vibration on the horizontal axis is greater than the vibration on the axial axis. The two vibration signals in the time domain are then processed using the STFT method.

3. RESULT AND DISCUSSION

3.1. FFT Computational Results

The calculation process is carried out using the FFT algorithm as shown by Equation 1. The graphs of the results of the FFT algorithm for measuring axial and radial positions are shown in Figures 9 and 10. Figure 9 shows a graph of the spectrum of the results of FFT processing at the axial measurement points. Because the input data comes from a non-stationary vibration signal, it produces many amplitude lines that appear evenly at a frequency of 0 –

40 Hz. The amplitude value becomes very small, and it is not clear which frequency value has the largest amplitude.

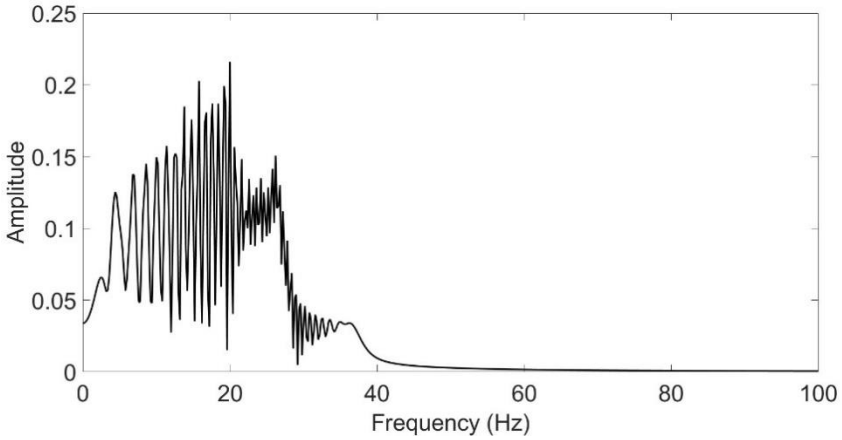

Figure 7. Axial spectrum

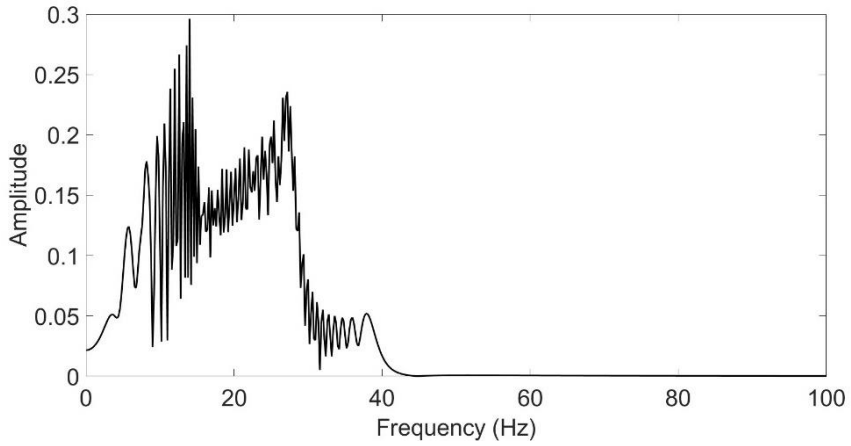

Figure 8. Horizontal spectrum

The spectrum graph of the results of processing the vibration signal on the horizontal axis using the FFT method is shown in Figure 8. The resulting spectrum shows the same characteristics as the vibration signal on the axial axis. It is also clear that both have the same characteristics before signal processing using the FFT method. The results of FFT processing show that the amplitude is evenly distributed in the 0 – 40 Hz frequency.

3.2. Time Domain Slicing Results

The results of cutting the time domain data are shown in Figures 9 and 10. Figure 9 shows a graph of the vibration signal in the time domain of the measurement results at the axial point. While the graph of the vibration signal in the time domain of the measurement results at the radial point is shown in Figure 10. These two-time domain graphs are the same as the graph data shown in Figures 5 and 6, the difference only lies in the reduced time. The previous graph had a time of 5 seconds and was reduced to 2 seconds. Signal cutting is done in the middle and symmetry.

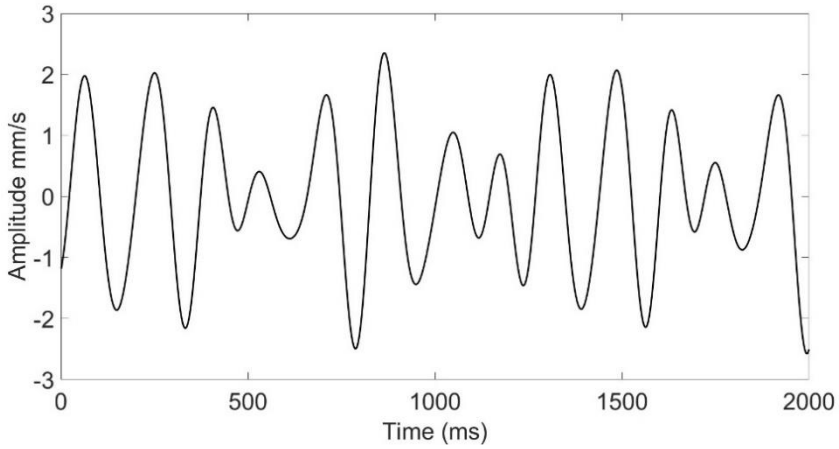

Figure 9. The result of cutting the time domain in the axial axis

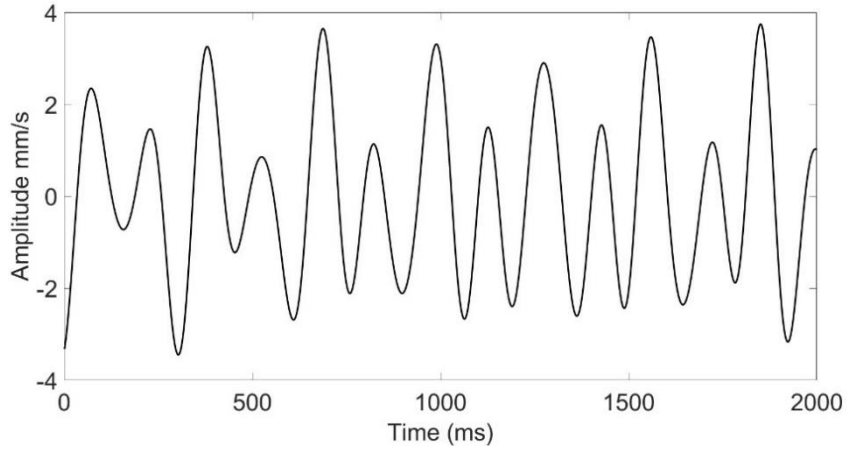

Figure 10. The result of cutting the time domain in the horizontal axis

3.3. Multiplication result of cutting time signal with Hanning window

Figures 11 and 12 are the result of multiplying the vibration signal in the time domain with the Hanning window. The multiplication of the Hanning window by the vibration signal from the axial point measurement is shown in Figure 11. The result of multiplying the vibration signal of the horizontal point measurement with the Hanning window is shown in Figure 12. This type of filter window is a filter that has a response to pass signals with frequencies above the cut off frequency and dampen signal that has a frequency below the cut-off frequency. So, it can be seen on both graphs that the amplitude value changes to 0 at the beginning and end of the signal. This result is in accordance with Figure 1 which has a value of 0 at each end and the largest amplitude is in the middle.

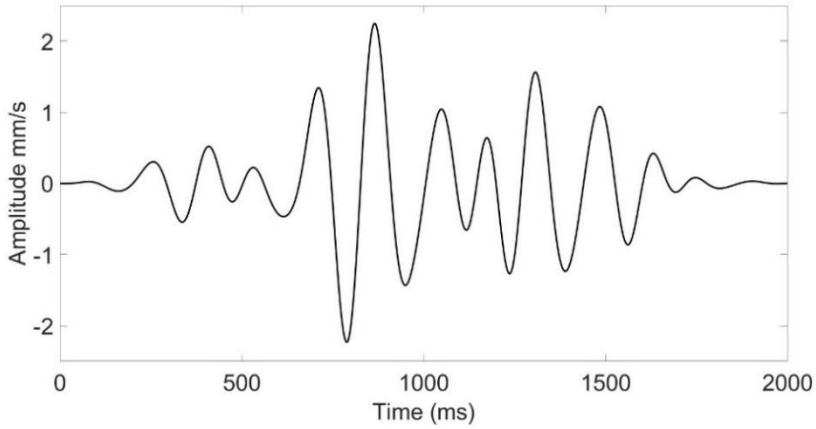

Figure 11. Axial time signal and Hanning window multiplication

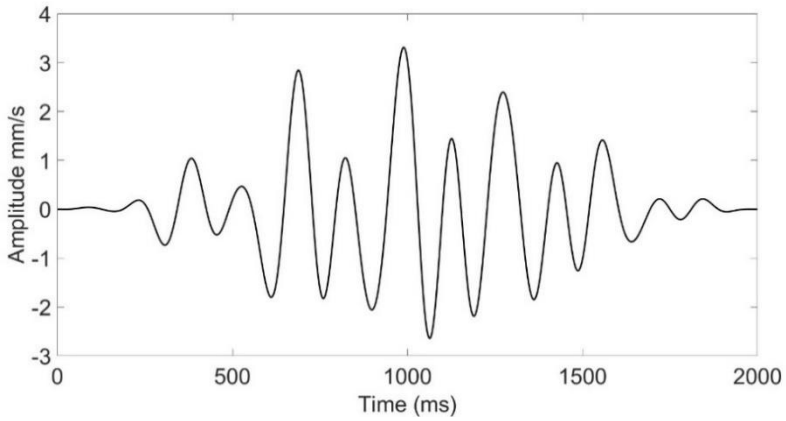

Figure 12. Horizontal time signal and Hanning window multiplication

3.4. Analysis of Spectrogram

After being cut and multiplied by the Hanning window function, the feature will be extracted using the STFT method. The extracted values in this study are the STFT value, the average amplitude of a signal, the frequency value and the time value when the amplitude is highest. These four values are used because the STFT method produces a time and frequency value, as well as an amplitude. The four values are used because the STFT method produces a time and frequency value, as well as an amplitude. STFT value is a complex number consisting of real and imaginary numbers that represent a value in the time and frequency domains. In order for the complex value to be calculated, the value is absolute.

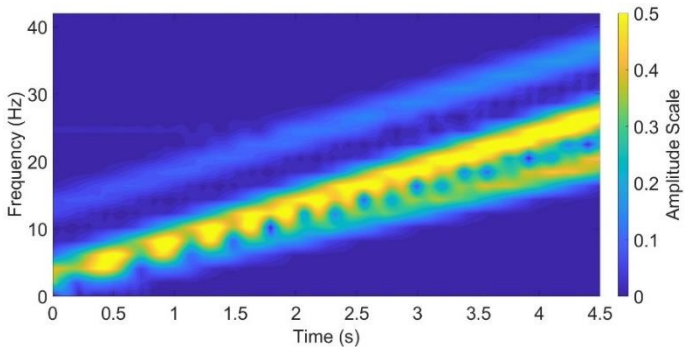

Figure 13. Axial spectogram

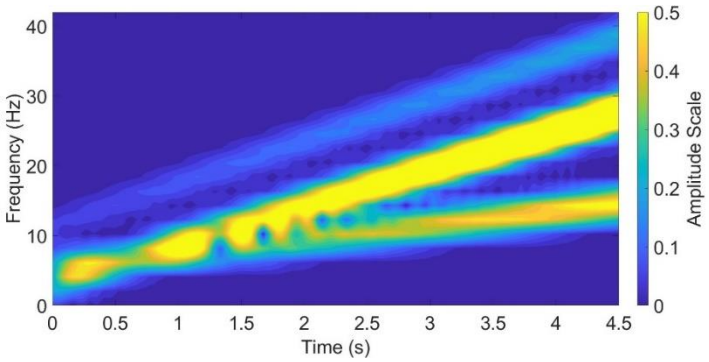

Figure 14. Horizontal spectrogram

The results of the STFT algorithm for the IDF vibration signal are shown in Figures 13 and 14, where the vibration frequency parameters are plotted against time. A spectrogram is a visual representation of sound in two-dimensional form, which illustrates the relationship of frequency with time, the amplitude of which is only approximated by the brightness of the color. Vibration amplitude is represented by yellow color degradation which means large amplitude value and blue color means small amplitude value. The results of the spectrogram in Figure 13 show that there are three high amplitudes at the final frequencies at values of 14 Hz, 25 Hz, and 37 Hz. The characteristics of this spectrogram have different meanings from the data generated by the FFT algorithm. In the graph, the results of FFT processing do not clearly show where the frequency is. The yellow area is mostly at a frequency of 25 Hz or equal to 1500 rpm. Where 1500 rpm is the rotational speed of the IDF motor. Based on existing references, this pattern indicates that the IDF is experiencing unbalance damage. Besides that, there is a little yellow color that is also scattered in some areas that are sourced from noise.

Figure 14 shows the density of the dominant yellow color being at the frequencies of 10 Hz, 25 Hz, and 37 Hz. Because in the vibration signal data there is little noise so that some amplitudes are also found in the spectrogram outside of the dominant frequency area. All spectra and spectrograms show the dominant frequency at 25 Hz or one rotational speed of the IDF, this confirms the results of the diagnosis of IDF damage as unbalance. If you refer to Figure 6 and the ISO 10816-3 velocity standard, the vibration value is included in the category of machines that can still operate but for a limited time.

4. CONCLUSION

The FFT and STFT methods were successfully applied to the IDF vibration signal which was originally in the form of a time domain into a spectrum and spectrogram. FFT produces a spectrum graph with evenly distributed amplitude values at a frequency of 0 – 40 Hz. The amplitude and frequency values cannot be read clearly if the processed vibration signal is a non-stationary signal. STFT processing results can be more legible when compared to FFT. The results of the spectrogram graph show the dominant IDF amplitude at a frequency of 25 Hz or one rotational speed of the IDF. This characteristic indicates an unbalance damage to the IDF with the largest vibration value of 3.7 mm/s RMS. When referring to the ISO 10816-3 velocity vibration standard, the IDF can still be operated in a short period of time. It is recommended to balance the IDF impellers to reduce vibration.

REFERENCES

[1] F. Anggara, D. Romahadi, A. L. Avicenna, and Y. H. Irawan, "Numerical analysis of the vortex flow effect on the thermal-hydraulic performance of spray dryer," SINERGI, vol. 26, no. 1, pp. 23–30, Feb. 2022, doi: 10.22441/SINERGI.2022.1.004.

[2] C. S. A. Gong Et Al., "Design and implementation of acoustic sensing system for online early fault detection in industrial fans," J. Sensors, vol. 2018, 2018, doi: 10.1155/2018/4105208.

[3] N. Dileep, K. Anusha, C. Satyaprathik, B. Kartheek, and K. R. A. Proffesor, "Condition Monitoring of FD-FAN Using Vibration Analysis," Int. J. Emerg. Technol. Adv. Eng., vol. 3, no. 1, pp. 170–186, 2013.

[4] S. Patidar and P. K. Soni, "An Overview on Vibration Analysis Techniques for the Diagnosis of Rolling Element Bearing Faults," Int. J. Eng. Trends Technol., vol. 4, no. 5, pp. 1804–1809, 2013.

[5] D. Romahadi, A. A. Luthfie, and L. B. D. Dorion, "Detecting classifier-coal mill damage using a signal vibration analysis," SINERGI, vol. 23, no. 3, pp. 175–183, Sep. 2019, doi: 10.22441/SINERGI.2019.3.001.

[6] D. Romahadi, F. Anggara, A. F. Sudarma, and H. Xiong, "The implementation of artificial neural networks in designing intelligent diagnosis systems for centrifugal machines using vibration signal," SINERGI, vol. 25, no. November 2020, 2021, doi: 10.22441/sinergi.2021.1.012.

[7] D. Romahadi, A. A. Luthfie, W. Suprihatiningsih, and H. Xiong, "Designing expert system for centrifugal using vibration signal and Bayesian Networks," Int. J. Adv. Sci. Eng. Inf. Technol., vol. 12, no. 1, p. 23, Jan. 2022, doi: 10.18517/IJASEIT.12.1.12448.

[8] D. Romahadi, H. Xiong, and H. Pranoto, "Intelligent system for gearbox fault detection & diagnosis based on vibration analysis using Bayesian Networks," IOP Conf. Ser. Mater. Sci. Eng., vol. 694, no. 1, 2019, doi: 10.1088/1757-899X/694/1/012001.

[9] G. Manhertz and A. Bereczky, "STFT spectrogram based hybrid evaluation method for rotating machine transient vibration analysis," Mech. Syst. Signal Process., vol. 154, p. 107583, Jun. 2021, doi: 10.1016/J.YMSSP.2020.107583.

[10] D. Romahadi, D. Feriyanto, W. Suprihatiningsih, and W. N. Setiawan, "Perancangan sistem diagnosis getaran motor menggunakan jaringan saraf tiruan propagasi mundur," J. Rekayasa Mesin, vol. 13, no. 1, pp. 37–46, Jun. 2022, doi: 10.21776/UB.JRM.2022.013.01.5.

[11] B. Hu and B. Li, "Blade crack detection of centrifugal fan using adaptive stochastic resonance," Shock Vib., vol. 2015, 2015, doi: 10.1155/2015/954932.

[12] Z. Gao, S. Member, C. Cecati, F. Ieee, and S. X. Ding, "IEEE Transactions on Industrial Electronics A Survey of Fault Diagnosis and Fault - Tolerant Techniques Part I : Fault Diagnosis with Model - Based and Signal - Based Approaches," vol. 62, pp. 3757–3767, 2015.

[13] K. Mollazade, H. Ahmadi, M. Omid, and R. Alimardani, "Vibration-Based Fault Diagnosis of Hydraulic Pump of Tractor Steering System by Using Energy Technique," Mod. Appl. Sci., vol. 3, no. 6, 2009, doi: 10.5539/mas.v3n6p59.

[14] C. Mateo and J. A. Talavera, "Short-Time Fourier Transform with the Window Size Fixed in the Frequency Domain (STFT-FD): Implementation," SoftwareX, vol. 8, pp. 5–8, 2018, doi: 10.1016/j.softx.2017.11.005.

[15] R. Dutta, J. P. Dwivedi, V. P. Singh, and A. Ghosh, "Using Vibration Analysis to Identify & Correct an Induced Draft Fan ' s Foundation Problem of a Pollution Control Device - A Case Study," Int. J. Appl. Eng. Res., vol. 13, no. 8, pp. 5831–5840, 2018.

[16] S. R. Vippala, S. Bhat, and A. A. Reddy, "Condition monitoring of BLDC motor using short time fourier transform," 2021 IEEE 2nd Int. Conf. Control. Meas. Instrumentation, C. 2021 - Proc., no. Cmi, pp. 110–115, 2021, doi: 10.1109/CMI50323.2021.9362938.

[17] C. T. Alexakos, Y. L. Karnavas, M. Drakaki, and I. A. Tziafettas, "A Combined Short Time Fourier Transform and Image Classification Transformer Model for Rolling Element Bearings Fault Diagnosis in Electric Motors," Mach. Learn. Knowl. Extr., vol. 3, no. 1, pp. 228–242, 2021, doi: 10.3390/make3010011.

[18] D. Mokrzan and G. Szymański, "Time-frequency methods of non-stationary vibroacoustic diagnostic signals processing," Rail Veh., no. 3, pp. 44–57, 2021, doi: 10.53502/rail-143047.

[19] L. Sandrolini and A. Mariscotti, "Impact of short-time fourier transform parameters on the accuracy of EMI spectra estimates in the 2-150 kHz supraharmonic interval," Electr. Power Syst. Res., vol. 195, no. July 2020, 2021, doi: 10.1016/j.epsr.2021.107130.

[20] V. Dekys, P. Kalman, P. Hanak, P. Novak, and Z. Stankovicova, "Determination of Vibration Sources by Using STFT," Procedia Eng., vol. 177, pp. 496–501, Jan. 2017, doi: 10.1016/J.PROENG.2017.02.251.

[21] F. Jurado and J. R. Saenz, "Comparison between discrete STFT and wavelets for the analysis of power quality events," Electr. Power Syst. Res., vol. 62, no. 3, pp. 183–190, Jul. 2002, doi: 10.1016/S0378-7796(02)00035-4.

[22] W. Jiang, X. Wu, Y. Wang, B. Chen, W. Feng, and Y. Jin, "Time-frequency-analysis-based blind modulation classification for multiple-antenna systems," Sensors (Switzerland), vol. 21, no. 1, pp. 1–19, 2021, doi: 10.3390/s21010231.

[23] A. Jablonski and K. Dziedziech, "Intelligent spectrogram – A tool for analysis of complex non-stationary signals," Mech. Syst. Signal Process., vol. 167, p. 108554, Mar. 2022, doi: 10.1016/J.YMSSP.2021.108554.